OPEN

Cognitive Severity-Specific Neuronal Degenerative Network in Charcoal Burning Suicide-Related Carbon Monoxide Intoxication

A Multimodality Neuroimaging Study in Taiwan

Nai-Ching Chen, MD, Chi-Wei Huang, MD, Shu-Hua Huang, MD, Wen-Neng Chang, MD, Ya-Ting Chang, MD, Chun-Chung Lui, MD, Pin-Hsuan Lin, MSc, Chen-Chang Lee, MSc, Yen-Hsiang Chang, MD, and Chiung-Chih Chang, MD, PhD

Abstract: While carbon monoxide (CO) intoxication often triggers multiple intraneuronal immune- or inflammatory-related cascades, it is not known whether the pathological processes within the affected regions evolve equally in the long term. To understand the neurodegenerative networks, we examined 49 patients with a clinical diagnosis of CO intoxication related to charcoal burning suicide at the chronic stage and compared them with 15 age- and sex-matched controls. Reconstructions of degenerative networks were performed using T1 magnetic resonance imaging, diffusion-tensor imaging, and fluorodeoxyglucose positron emission tomography (PET). Tract-specific fractional anisotropy (FA) quantification of 11 association fibers was performed while the clinical significance of the reconstructed structural or functional networks was determined by correlating them with the cognitive parameters. Compared with the controls, the patients had frontotemporal gray matter (GM) atrophy, diffuse white matter (WM) FA decrement, and axial diffusivity (AD) increment. The patients were further stratified into 3 groups based on the cognitive severities. The spatial extents within the frontal-insular-caudate GM as well as the prefrontal WM AD increment regions determined the cognitive severities among 3 groups. Meanwhile, the prefrontal WM FA values and PET signals also correlated significantly with the patient's Mini-Mental State Examination score. Frontal hypometabolic patterns in PET analysis, even after adjusted for GM volume, were highly coherent to the GM atrophic regions, suggesting structural basis of functional alterations. Among the calculated major association bundles, only the anterior thalamic radiation FA values correlated significantly with all chosen cognitive scores. Our findings suggest that fronto-insular-caudate areas represent target degenerative network in CO intoxication. The topography that occurred at a cognitive severity-specific level at the chronic phase suggested the clinical roles of frontal areas. Although changes in FA are also diffusely distributed, different regional changes in AD suggested unequal long-term compensatory capacities among WM bundles. As such, the affected WM regions showing irreversible changes may exert adverse impacts to the interconnected GM structures.

(*Medicine* 94(19):e783)

Abbreviations: AD = axial diffusivity, CO = carbon monoxide, FA = fractional anisotropy, GM = gray matter, MMSE = Mini-Mental State Examination, MRI = magnetic resonance imaging, PET = positron emission tomography, SUVr = standard uptake value ratio, WM = white matter.

INTRODUCTION

Every year, about a million people take their own lives with methods differ from place to place. While hanging is the predominant suicide method in many countries, there has been a rapid rise in suicide by inhalation of barbecue charcoal gas in Taiwan since 2001, before which this method of suicide was very rare.[1] A study conducted from 1995 to 2011 reported a marked increase in charcoal-burning suicides in Taiwan and Hong Kong.[2] As this has not been reported in other East or Southeast Asian countries, this phenomenon may represent differences in regional culture or media portrayal. Survivors often experienced acute, delayed, and chronic neuropsychiatric complications[3] related to carbon monoxide (CO) intoxication. Toxic exposure to CO may trigger multiple downstream stress responses that included inflammation, hypoxia, and oxidative stress reactions.[4–9] The stress responses in CO intoxication are continuous which depend on the immune or inflammatory responses of the subject.[10] Neuronal necrosis in the acute phase and apoptosis in the delayed phase have been demonstrated in a translational model,[11] which is consistent with postmortem findings in human.[12]

At the acute CO intoxication phase, diffuse white matter (WM) damages are well reported. In contrast, little is known systemically regarding the long-term evolution of these injuries. From a neuroimaging perspective, the affected WM bundles may undergo reversible[4–9] or irreversible changes.[6,13] Whether the initial damaged WM bundles compensate equally at the chronic phases or they may undergo selective patterns of neurodegeneration required to be explored. The gray matter

Editor: Robert Barkin.
Received: February 17, 2015; revised: March 10, 2015; accepted: March 23, 2015.
From the Cognition and Aging Center (N-CC, C-WH, W-NC, Y-TC, C-CC), Department of Neurology; Department of Nuclear Medicine (S-HH, Y-HC); Department of Radiology (C-CL, C-CL), Kaohsiung Chang Gung Memorial Hospital, Chang Gung University College of Medicine; and Department of Health and Beauty (P-HL), Shu-Zen College of Medicine and Management, Kaohsiung, Taiwan.
Correspondence: Chiung-Chih Chang, Department of Neurology, Kaohsiung Chang Gung Memorial Hospital and Chang Gung University College of Medicine, Kaohsiung, Taiwan, #123, Ta-Pei Road, Niaosung, Kaohsiung County 833, Taiwan (e-mail: neur099@adm.cgmh.org.tw).
This work was supported by grants CMRPG8A0511, CMRPG 8B1001 and CMRPG8C041 from the Chang Gung Memorial Hospital and NSC 102–2314-B-182A-059 and 103–2314-B-182A-034 from the National Science Council to C.C.C.
The authors have no conflicts of interest to disclose.

ISSN: 0025-7974
DOI: 10.1097/MD.0000000000000783

(GM) damages often developed in a latent periods compared with the WM changes and the reported areas included the striatum,[14] globus pallidus,[15] hippocampus,[16] frontal cortex,[17] and anterior cingulate cortex.[14] Whether changes in GM reflect topography of interconnected WM injuries is also not known.

There is a growing interest in monitoring pathological status using functional neuroimaging, as the alterations are sensitive and often precede morphological changes. The largest series using fluorodeoxyglucose positron emission tomography (PET) in CO intoxication was published in 1989 and describes the behavioral patterns of 8 patients.[18] In this report, 7 patients had hypometabolism of the prefrontal cortex.[18] Other reports using PET have been limited to case series focusing on visual loss,[19–21] akinetic mutism,[22] and Parkinsonian features.[23]

A functional neuroimaging survey without structural quantification may not provide sufficient information to understand whether the changes in functional patterns be related to local structural alterations, distant diaschisis, or both. As such, magnetic resonance imaging (MRI) provides structural context in complementary that reflects brain modifications after disease processes. Through assessing tissue microstructure by mapping water proton motions,[24] current MRI technology has made possible the in vivo assessment of WM integrity by using diffusion-tensor imaging. Fractional anisotropy (FA) is a diffusion-tensor imaging–derived parameter that quantifies the directionality and coherence of the WM tracts; it is believed to represent such factors as myelination, axonal density, and/or integrity.[25] An increased axial diffusivity (AD) has been attributed to axonal changes in patients with CO intoxication.[8] The development of WM parcellation algorithm allows approximating the 3D trajectories of major WM bundles by probabilistic maps[26] that allows for fiber integrity estimation. With automated tract-specific quantification of FA, the lesion-tract correlation study can be performed. This technique could therefore help shed more light on the linkage between the target association fiber pathways and the clinical weightings on the cognitive profiles. In addition, by multiparametric neuroimaging comparisons, the long-term impact of nonphysiological stress reactions in CO intoxication can be modeled, and answer the structural-functional relationships.

To date, proof-of-concept experiments to establish the neuronal vulnerability networks in CO intoxication patients are lacking, and it is not known whether the cerebral structures that undergo decompensatory processes appear randomly or represent specific injury patterns that also determine the cognitive severity. We hypothesized that intracellular stress responses triggered by a single toxic exposure to CO may result into a later phase degenerative network that is cognitive severity specific, and that the spatial extent of the network may represent regions where the salvage system fails to compensate. An understanding of the affected anatomical locations may offer insights into other diseases showing similar pathophysiologic mechanisms.

Based on the aim of this study, only CO intoxication patients in the chronic phase were enrolled. For neuroimaging parameters, we included brain MRI and PET for structural and functional map reconstructions. GM atrophy and increases in AD represented irreversible neuroimaging biomarkers, in contrast to FA, which indicated possibly reversible demyelinating changes. It is generally accepted that regional atrophy has a significant impact on PET image quality and quantitative accuracy.[27] Therefore, the PET signals were corrected for a partial volume effect. The clinical significance of the identified network was determined by analyzing the structural-functional and network-cognitive test score relationships.

MATERIAL AND METHODS

This study was approved by the Institutional Review Board of Chang Gung Memorial Hospital, and the experiments were undertaken with the written, informed consent of each subject or their caregiver (where appropriate).

Patient Enrollment

This study was conducted at the neurology clinic of Kaohsiung Chang Gung Memorial Hospital in 2009. The clinical diagnosis of CO intoxication was made based on a history of a charcoal-burning suicide attempt and an elevated carboxyhemoglobin level (>10%) in the emergency room.[3] The exclusion criteria were an agitated mood or a confused state that prevented an accurate assessment of the patient's neuropsychiatric status.[28] The mean interval between CO intoxication and the study enrollment was more than 1.5 years (range 20–50 months). Forty-nine patients and 15 age- and gender-matched healthy subjects completed the study.

Cognitive Testing

General intellectual function was assessed using the Mini-Mental State Examination (MMSE).[29] Verbal and nonverbal episodic memory was assessed using the modified California Verbal Learning Test—Mental Status[30] and the Rey-Osterrieth Complex Figure Test after a 10-minute delay.[31] Language screening included the 16-item Boston Naming test,[32] and semantic verbal fluency tests. The subjects' visual-spatial abilities were assessed by a modified Rey-Osterrieth Complex Figure Test, and the number-location test from the Visual Object and Space Perception Battery.[33] Executive function was assessed using digit backward span, design fluency, Stroop Interference, and Modified Trails B tests.[34]

Grouping of the Patients According to Cognitive Severity

Cognitive severity was assessed by clinical dementia rating, since it scores the functional capacity of participants independently of physical disability.[8,35] All of the subjects were assigned a clinical dementia rating score as follows: 0 indicating no dementia, and 0.5, 1, 2, and 3 indicating questionable, mild, moderate, and severe dementia, respectively.[30] Patients with a clinical dementia rating score of 0 were defined as Group 1, a clinical dementia rating score of 0.5 as Group 2, and a score of 1 or 2 as Group 3. We did not select patients with a clinical dementia rating score of 3 because of a floor effect in the cognitive tests.

Fluorodeoxyglucose PET Acquisition

All of the images were obtained using an integrated PET/computed tomography system (Discovery ST, General Electric Medical System, Milwaukee, WI). A fasting glucose level <150 mg/dL was ensured prior to the imaging procedure. After an injection of 370 Mbq of ^{18}F-fluorodeoxyglucose, the patients were placed in a quiet, dimly lit environment with minimal background noise, where they stayed for 40 minutes. Helical computed tomography images were acquired first using the following parameters: 140 kV, 170 mA (maximum), and 3.75-mm-thick sections. A single PET/computed tomography image of the head region was then taken for 10 minutes and

reconstructed using an ordered subsets expectation maximization algorithm (2 iterations, 30 subsets; Gaussian filter: 2 mm) with computed tomography–based attenuation correction. The reconstructed images were characterized by a matrix size of 256×256 and a voxel size of $1.2 \times 1.2 \times 3.25\,mm^3$.

Fluorodeoxyglucose PET Analysis

PET images were first coregistered to the corresponding MRI, and individual MRI were spatially normalized to the Montreal Neurological Institute template with a voxel size of the written normalized images of $2 \times 2 \times 2\,mm^3$ with default estimation and writing options. Each PET image was then corrected for partial volume effect.[36] The spatial normalization parameters were then applied to the corresponding partial-volume corrected PET image to obtain the final normalized PET image in the Montreal Neurological Institute domain. The occipital GM was considered the reference region.[14]

Voxel-wise analysis of the standard uptake value ratio (SUVr) parametric image was performed using Spatial Parametric Mapping Version 8 software (Wellcome Department of Cognitive Neurology, Institute of Neurology, London, UK). We calculated between-group differences using nonparametric voxel-wise analysis (SnPM13; http://warwick.ac.uk/snpm) after $8 \times 8 \times 8\,mm^3$ variance smoothing with 5000 permutations. The significance threshold was set at $P < 0.01$, corrected for multiple comparisons across the entire brain (the false discovery rate) with an extended threshold of 250 voxels.

Structural Imaging for GM and WM Analyses

3D T1-weighted MR images[37] were obtained for each subject for GM atrophy nonparametric voxel-wise analysis. Age and gender were considered to be covariates of no interest to exclude their possible effects on regional GM volume.[38] The significance threshold was set at $P < 0.01$, corrected for multiple comparisons across the entire brain (the false discovery rate) with an extended threshold of 250 voxels.

Sixty-one direction diffusion tensor images were acquired for FA and AD map calculations[39] and tract-based spatial statistics for postprocessing analysis (FSL version 4.0.1 package, http://www.fmrib.ox.ac.uk). A restrictive statistical threshold was used (threshold-free, cluster-enhancement threshold with $P < 0.05$, corrected for multiple comparisons). A WM parcellation algorithm with automated tract-specific quantification of 11 major WM bundles by probabilistic maps was used.[26] The mean FA of each WM bundle was calculated for correlation purposes.

TABLE 1. Demographic Data of the Carbon Monoxide Intoxication Patients and Controls

	Age-Matched Controls (n = 15)	All Patients (n = 49)	Group 1 Patients CDR = 0 (n = 12)	Group 2 Patients CDR = 0.5 (n = 21)	Group 3 Patients CDR ≧1 (n = 16)
Age (y)	41.0 ± 6.6	42.7 ± 10.6	39.5 ± 9.4	43.7 ± 10.5	43.7 ± 11.8
Gender (male/female)	8 / 7	19 / 30	6 / 6	9 / 12	4 / 12
Education (ye)	15.0 ± 3.7	13.8 ± 4.2	12.4 ± 3.4	12.7 ± 4.3	14.6 ± 4.4
Initial carboxyhemoglobin (%) (mean, range)	–	37.3 %, 14–75	32.4%,15–69	38.5%,14–70	37.9%,12–73
Mini-Mental State Examination	28.8 ± 0.9	21.8 ± 9.1*	28.8 ± 1.4	25.6 ± 3.5	10.1 ± 7.5*,†,‡
Verbal memory: CVLT-MS (9)					
4 Learning trials	30.7 ± 3. 9	22.8 ± 8.6*	30.4 ± 2.8	23.1 ± 6.5*,†	13.1 ± 7.8*,†,‡
30-s free recall	8.3 ± 0.98	5.8 ± 2.9*	8.3 ± 1.2	6.0 ± 2.2*,†	2.6 ± 2.6*,†,‡
10-min free recall	8.2 ± 1.4	5.5 ± 3.1*	8.3 ± 1.1	5.4 ± 2.7*,†	2.4 ± 2.6*,†,‡
Correct after cues	8.3 ± 1.2	5.4 ± 3.1*	7.9 ± 1.2	5.3 ± 2.6*,†	2.6 ± 3.1*,†,‡
Correct word recognition	8.7 ± 0.7	7.4 ± 2.2*	8.3 ± 1.1	7.7 ± 1.7	5.5 ± 3.0*,†
Visual memory					
Modified Rey-Osterrieth recall (17)	14.9 ± 2.3	9.3 ± 5.9*	12.4 ± 4.8	10.1 ± 5.2	4.0 ± 5.4*,†,‡
Visual spatial functions					
Modified Rey-Osterrieth copy (17)	17.0 ± 0.0	13.9 ± 5.7*	17.0 ± 0.0	14.7 ± 4.7	8.6 ± 7.7*,†,‡
Visual Object and Space Perception (10)	9.07 ± 1.28	6.9 ± 3.3*	9.1 ± 1.4	7.4 ± 2.4	3.4 ± 3.9*,†,‡
Speech and language ability					
Boston naming test (16)	15.6 ± 0.8	13.7 ± 3.7*	15.8 ± 0.6	14.5 ± 2.0	9.7 ± 5.5*,†,‡
Semantic fluency (fruit)	15.9 ± 3.4	10.2 ± 4.8*	13.9 ± 3.3	10.3 ± 3.8*	5.5 ± 4.1*,†,‡
Executive function					
Digit backward	5.8 ± 1.3	3.7 ± 1.8*	5.3 ± 1.5	3.6 ± 1.1*,†	2.1 ± 1.7*,†
Correct line in trail making (14)	13. 7 ± 0.9	9.9 ± 5.1*	13.2 ± 2.9	11.0 ± 3.6	3.1 ± 4.0*,†,‡
Trail-making completion time (s)	34.1 ± 25.0	66.8 ± 40.0*	36.2 ± 14.6	68.8 ± 40.6*	107.9 ± 23.6*,†
Stroop test	53.8 ± 10.1	30.0 ± 18.0*	42.7 ± 15.5	31.6 ± 14.7*	11.3 ± 11.7*,†,‡
Design fluency	9.9 ± 4.6	7.0 ± 4.2	9.2 ± 3.7	7.1 ± 3.7	3.9 ± 4.1*,†

Data are expressed as the mean ± standard deviation; number in parenthesis indicates maximal score. CDR = clinical dementia rating, CVLT-MS = California Verbal Learning Test—Mental Status.

* $P < 0.01$, compared with the controls.

† $P < 0.01$ compared with Group 1.

‡ $P < 0.01$ compared with Group 2.

Statistical Analysis

Categorical variables were compared using the χ^2 test. The Kruskal-Wallis H-test was used to compare the neuropsychiatric performance between groups, as these data were not normally distributed. Pearson correlation was used to explore the relationships between continuous variables. All statistical analyses were performed using SPSS software (version 11.0 for Windows; SPSS, Chicago, IL), and a P value less than 0.05 (2 tailed) was considered to be statistically significant.

For structural-functional relationships, multivariate linear regression analysis was used to test the independent associations between the regions showing hypometabolism in PET as a predictor of the WM FA value. The selected regional variables in the regression model were based on the PET findings showing significant differences between the patients and controls. The nuisance variable was the age of the patient. We used a threshold-free, cluster-enhancement threshold with $P < 0.05$ for statistical significance.

Multivariate linear regression analysis was also used to test the independent associations between regional SUVr as a predictor of cognitive performance. Age and educational level were considered to be the nuisance variables. The R^2 value represented the goodness of fit to the regression model, and a P value less than 0.05 (2 tailed) was considered to be statistically significant.

RESULTS

Demographic Data and Cognitive Test Comparisons

The cognitive performance and demographic data of the patients and controls are listed in Table 1. While there was no difference in cognitive performance between the patients in Group 1 and the controls, Group 2 patients had impaired verbal memory and executive function scores compared with the controls and Group 1 patients. The cognitive scores were significantly lower in Group 3 compared with the controls, Group 1 or Group 2.

Structural and Functional Networks Targeted at the Anterior Brain Regions (Figure 1)

For the 49 patients, both GM atrophy (Figure 1A) and PET hypometabolism pattern (Figure 1B) pointed to anterior brain regions including the medial prefrontal region, orbital prefrontal, dorsolateral prefrontal, posterior cingulate cortex, anterior insular, anterior temporal, caudate nucleus, and thalamus. Although the PET signals were adjusted for regional volume atrophy, the spatial extent was more confluent and overlapped with the GM atrophic maps in the dorsal-medial and dorsal-lateral prefrontal cortex and insular regions. Of specific notes, the temporal-parietal and posterior cingulate cortex represented 2 isolated clusters in PET located in the posterior brain regions. Increased AD was found diffusely distributed in the long-association fiber tracts (Figure 1C, red clusters) as well as in the frontal U fibers (Figure 1C, arrows).

Topographic Changes Related to Cognitive Severity

We then compared the structural and functional spatial distribution in the 3 patient groups. In Group 1, GM atrophy (Figure 2A1) was found in the anterior cingulate cortex (sagittal view), caudate, anterior insular regions, and temporal-parietal

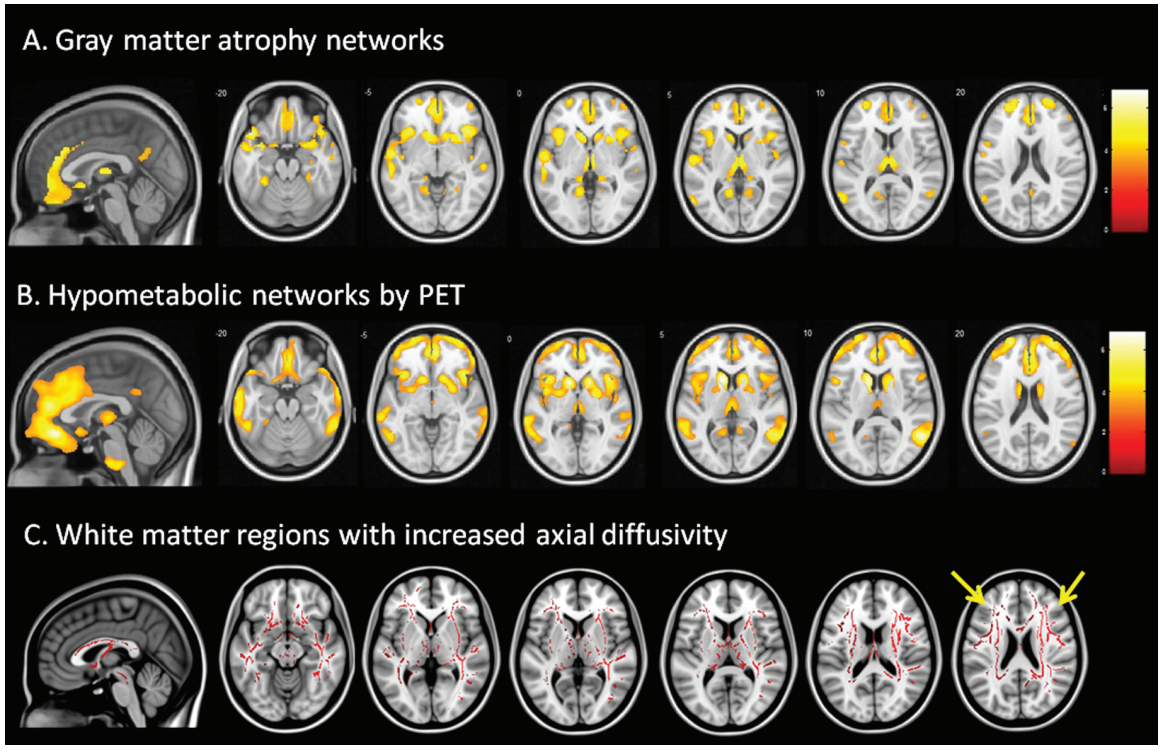

FIGURE 1. Voxel-wise comparisons between the controls and patients for (A) gray matter atrophy (B) hypometabolism of fluorodeoxyglucose positron emission tomography (PET) (C) and increased axial diffusivity. Figure 1C arrow = frontal U fibers. The background anatomic reference = MNI 152 T1 image.

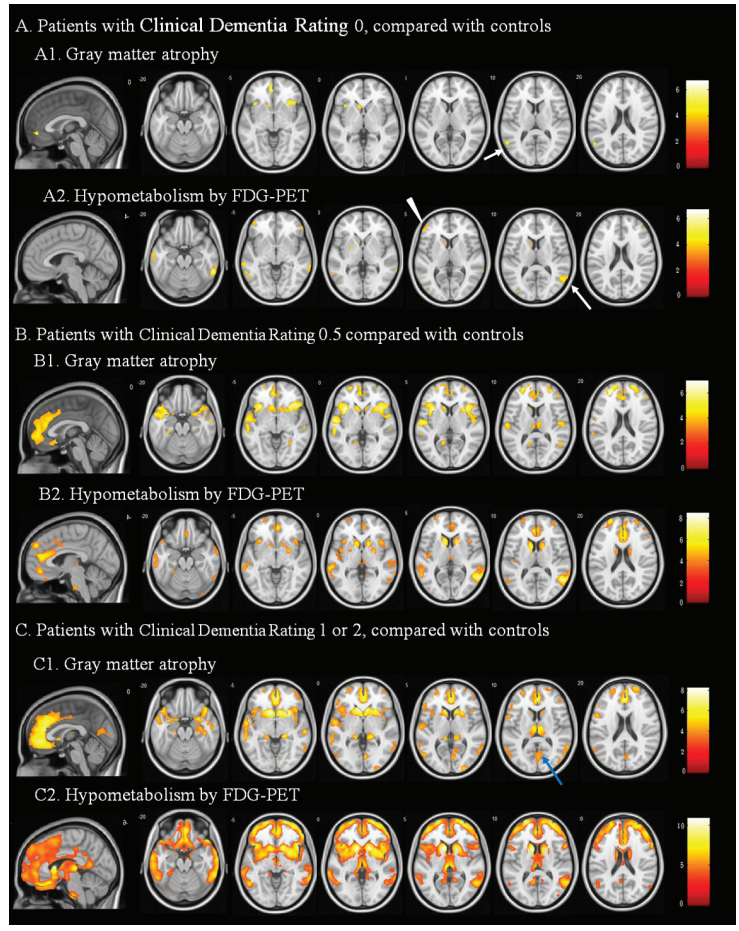

FIGURE 2. Comparison of gray matter atrophy and hypometabolism by fluorodeoxyglucose positron emission tomography (FDG-PET) in the patients stratified by clinical dementia rating score: (A) clinical dementia rating 0; (B) clinical dementia rating 0.5; (C) clinical dementia rating ≧1. Figure A1 arrow = temporal-parietal cortex, arrow head = dorsolateral prefrontal cortex, Figure A2 arrow = temporal-parietal cortex, Figure C1 arrow = posterior cingulate cortex.

junction (Figure 2A1, arrow). Hypometabolism was noted in the dorsolateral prefrontal areas (Figure 2A2, arrow head) and temporal-parietal regions (Figure 2A2, arrow). In Group 2, the atrophic areas (Figure 2B1) included bilateral medial and dorsolateral prefrontal areas, caudate, anterior insular, and thalamus. The hypometabolism regions in Group 2 (Figure 2B2) corresponded to the atrophic regions but to a wider extent in the temporal-parietal areas. The atrophic regions in Group 3 (Figure 2C1) covered all of the regions shown in Group 2 analysis and were more confluent in the frontal-striatum-thalamic, temporoparietal, and posterior cingulate regions (Figure 2C1, blue arrow). The hypometabolic regions in Group 3 involved the entire frontal-insular-striatum and thalamus, as well as the lateral temporal, temporal-parietal regions and posterior cingulate cortex (Figure 2C2). The percentage of SUVr decline among the identified regions compared with the controls is shown in Supplementary Table 1, http://links.lww.com/MD/A256.

For WM analysis (Figure 3), the significant regions showing decreased FA were diffusely distributed in all 3 patients groups (red clusters in Figure 3A: Group 1; 3B: Group 2; 3C: Group 3). For WM AD analysis, a transition of frontoanterior temporal to the occipital gradients according to cognitive severity (blue clusters in Figure 3A: Group 1; 3B: Group 2; 3C: Group 3) was found.

Frontal Cortical SUVr and WM FA Predicted the Cognitive Test Scores

The MMSE scores were significantly correlated with the prefrontal WM and the forceps minor FA (Figure 4A, green voxels). Correlations between the MMSE scores with cortical SUVr were found in the orbital-frontal and dorsolateral prefrontal regions, anterior insular, temporal-parietal, and posterior cingulate cortex (Figure 4B, arrow). There were no correlations between any GM partitions with MMSE scores.

Based on the PET findings, the SUVr values in the inferior frontal regions (automated anatomical labeling area 11–16) and lateral frontal regions (automated anatomical labeling area 3, 4, 7, 8) were further extracted and entered separately into the regression model to predict the related WM involvement. The inferior frontal region SUVr correlated with the FA values in the periaqueductal, forceps minor, anterior frontal regions and thalamus (Figure 4C). For the lateral frontal SUVr (Figure 4D), correlations were seen in the anterior frontal WM, anterior internal capsule, forceps major, thalamus, and the periaqueductal WM.

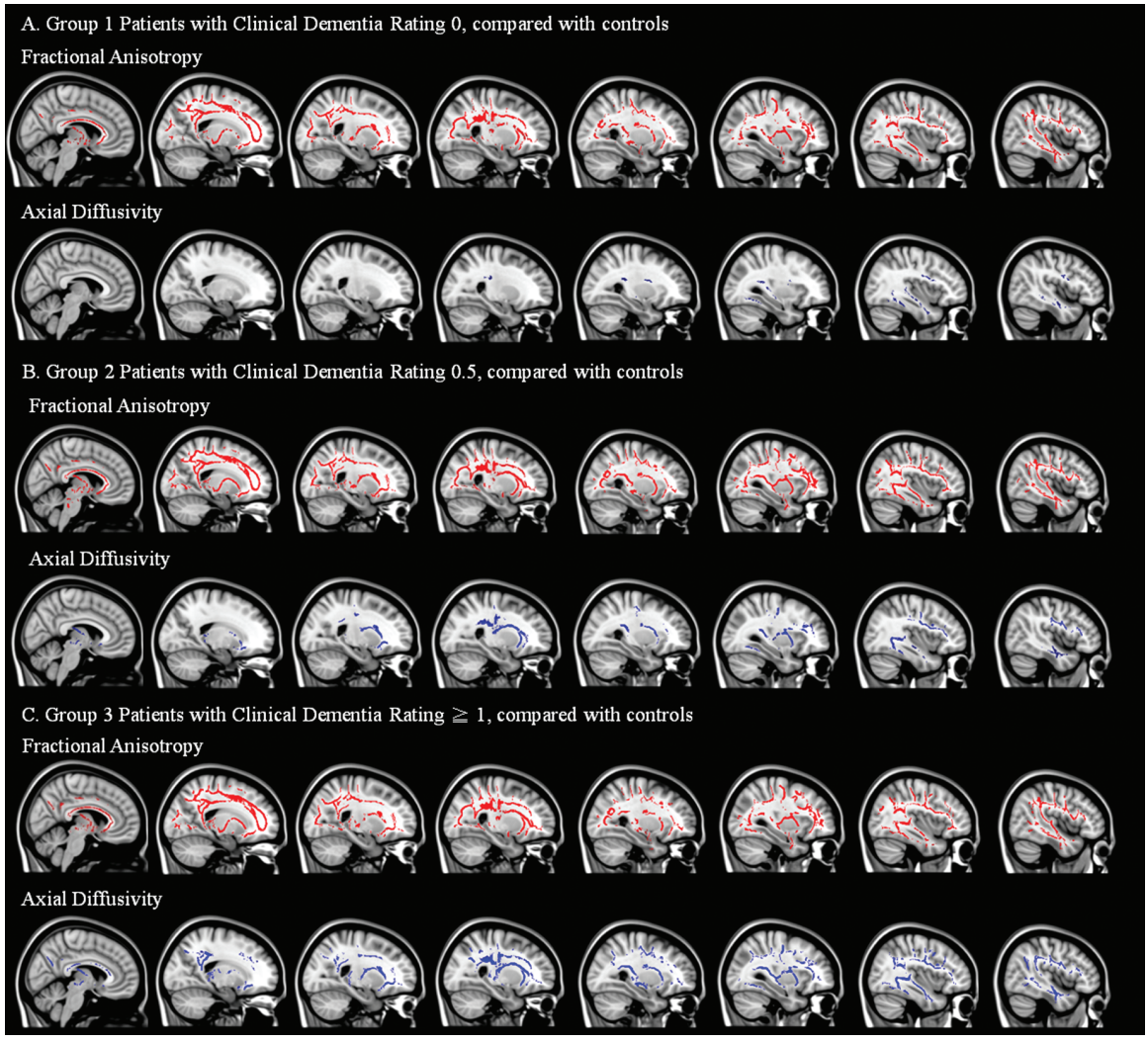

FIGURE 3. Changes in fractional anisotropy (red clusters) or axial diffusivity (blue clusters) in the patients stratified by clinical dementia rating score: (A) clinical dementia rating 0; (B) clinical dementia rating 0.5; (C) clinical dementia rating ≧1. The background anatomic reference = MNI 152 T1 image in a sagittal plane.

Figure 5 illustrates the scatter plots of the individual significant regions against the verbal memory learning scores (Figure 5A), Stroop test score (Figure 5B), digit backward score (Figure 5C), and clinical dementia rating sum of box score (Figure 5D). The SUVr values of the inferior and lateral frontal areas were consistently correlated with the selected tests.

Anterior Thalamic Radiation Integrity Was Crucial for the Prediction of Functional Anchored Network and Cognitive Test Scores

We calculated 11 major association fiber FA values and explored the relationships between the fiber FA values with the MMSE, verbal memory learning score, Stroop test score, and digit backward score (Table 2). While the forceps major, forceps minor, inferior frontooccipital fasciculus, superior longitudinal fasciculus, and uncinate fasciculus were separately related to individual test scores, only the anterior thalamic radiation correlated with all of the test scores.

DISCUSSION

Major Findings

Based on the physiological meaning of the selected imaging biomarkers, our study results support the initial hypothesis that a specific irreversible degenerative pattern, majorly seen in the anterior brain, represents a long-term decompensatory network in CO intoxication. The major findings here support the theme. First, we identified frontal-temporal GM atrophy as well as interconnected WM tracts AD values changes. While both parameters indicated irreversible changes, the structural changes were highly functionally anchored. Hypometabolic topography, corrected for regional atrophy, was highly coherent to the topography of GM atrophy suggesting local neuronal hypofunction rather than diaschisis effect. The relationships between prefrontal WM FA with the inferior or lateral prefrontal SUVr also suggested that prefrontal WM disruption may augment the regional hypometabolism where the fibers connect. Meanwhile, the spatial extents of the prefrontal GM and WM network explained both cognitive test scores and cognitive

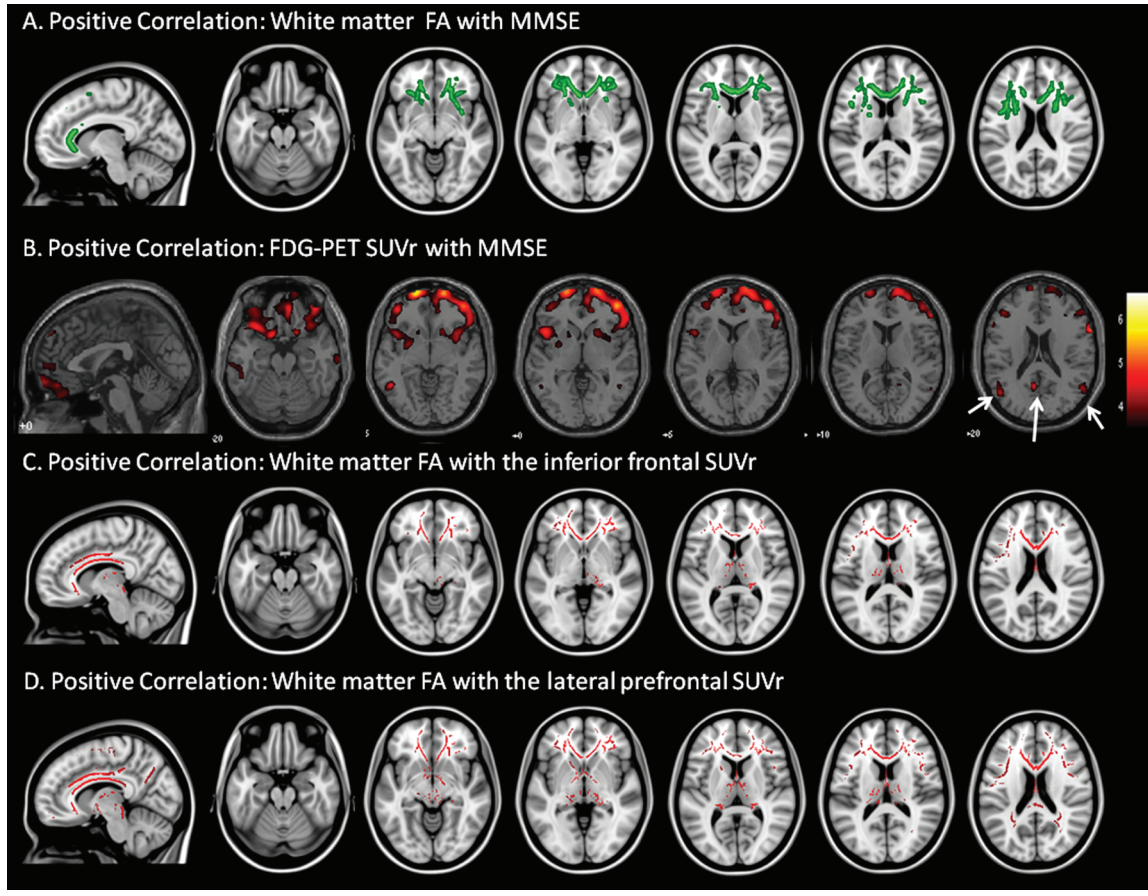

FIGURE 4. Correlation analysis between (A) white matter fractional anisotropy (FA) or (B) fluorodeoxyglucose positron emission tomography (FDG-PET) standard uptake value ratio (SUVr) with Mini-Mental State Examination (MMSE) score. Significant correlations between the white matter FA with the (C) inferior frontal regions and (D) lateral prefrontal region SUVr. Figure 4B arrow = temporoparietal and posterior cingulate region.

severity while the correlations between the parcellated tract FA values with cognitive tests also reenforced the importance of the major association fiber integrity.

Influence of Prefrontal WM Axonopathy to Interconnected GM

Our analysis provides a new understanding of the relationship between GM and WM in CO intoxication, although the upstream or downstream relationships between these 2 were still inconclusive. While WM is the most vulnerable anatomical structure at acute CO intoxication phase,[8] changes in GM are often found in a latent phase. Our study identified prefrontal GM atrophy with adjacent WM regions showing increased AD values. As such, the irreversible WM changes may augment the adjacent interconnected GM pathological processes via Wallerian degeneration. Meanwhile, we speculated the prefrontal axonopathy also eroded distantly connected posterior brain regions. The inferior frontooccipital fasciculus and superior longitudinal fascicules represent dense frontal fiber bundles that connect the posterior brain structures.[40] Both bundles are also of clinical importance in CO intoxication as they also bypass the disrupted prefrontal WM networks. Alternatively, damages in splenium may contribute to the posterior temporal-parietal and precuneus atrophy as shown in Group 3. Of note, the observed GM atrophy in this study could not be attributed to the normal aging process, since volumetric analysis was measured in a previously physically intact adult population with an average age of 42 years.

The structural integrity of prefrontal WM fibers that bypass the anterior horn of the ventricle is crucial for the functional integrity of interconnected frontal regions in CO intoxication. Via the anterior limb of the internal capsule and the fibers surrounding the anterior horn of the lateral ventricle, the anterior thalamic radiation connects the anterior and midline thalamus nuclei with the frontal lobe.[41] The anterior thalamic radiation was highlighted in this study compared to the other major association WM bundles not only because it bypassed the reported prefrontal WM regions. The integrity of the anterior thalamic radiation also explained all of the test scores.

Functional-Anchored Network That Determined Cognitive Outcomes

Structural connections among inferior frontal, lateral frontal, anterior cingulate cortex, and temporal cortex have been established,[42,43] as well as frontal injuries in CO intoxication.[3] However, no previous study has purposed the scattered frontal regions as a vulnerability network specific to CO intoxication. Our study results suggest that tissue vulnerability in CO

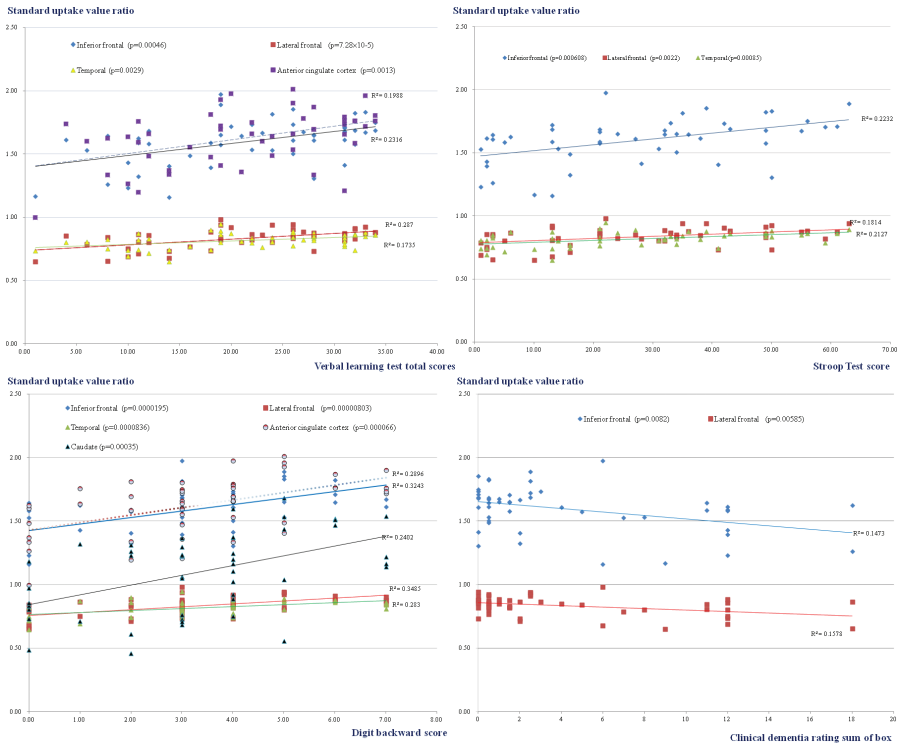

FIGURE 5. Regression model of the significant regional standard uptake ratio against verbal memory learning score (A), Stroop test score (B), digit backward score (C), and clinical dementia rating sum of box score (D).

intoxication occurs at a cognitive-severity–specific topography rather than being randomly distributed. Different brain regions may have unequal compensatory mechanisms to the stress cascades and our study results suggested lower capacities taking place at the anterior brain network.

Neuroimaging Changes in Patients Without Objective Cognitive Deficits

While it has been reported that people who survive initial CO insults usually recover within 6 months to 1 year,[44] evidence from cross-sectional,[14,28] longitudinal,[8,45,46] and the present study suggest long-lasting, and perhaps permanent, subtle to detectable neuroimaging changes. Of specific note, in our Group 1 patients without significant objective cognitive deficits, the structural changes were evidenced by diffuse decreases in FA and regional increases in AD. Recent studies in Alzheimer diseases have suggested earlier reflection of disease status using structural neuroimaging approaches[47] compared with the cognitive evaluation. The neuroimaging changes can be detected prior to the onset of clinical symptoms. Further studies with a longer observation period are needed in the

TABLE 2. Correlation Analysis Between Association Fibers and Cognitive Tests

Association Fiber Fractional Anisotropy Values	MMSE	Verbal Learning Test	Stroop Test	Digit Backward
Anterior thalamic radiation	0.351*	0.329*	0.326*	0.426†
Corticospinal tract	0.237	0.137	0.172	0.140
Cingulum (cingulate gyrus)	0.151	0.131	0.159	0.303
Cingulum (hippocampus)	0.057	−0.097	0.087	−0.116
Forceps major	0.372*	0.191	0.259	0.316*
Forceps minor	0.408†	0.221	0.316*	0.335*
Inferior frontooccipital fasciculus	0.385†	0.228	0.341*	0.242
Inferior longitudinal fasciculus	0.253	0.085	0.246	0.173
Superior longitudinal fasciculus	0.340*	0.208	0.239	0.189
Uncinate fasciculus	0.348*	0.228	0.142	0.104
Superior longitudinal fasciculus (temporal part)	0.294	0.105	0.199	0.079

Numbers indicated correlation coefficient, adjusted for age in the patients. MMSE = Mini-Mental State Examination, Verbal learning test using California Verbal Learning Test—Mental Status 4 learning trials scores.

* $P < 0.05$.

† $P < 0.01$.

asymptomatic patients to elucidate whether our neuroimaging results reflect nonspecific imaging changes in CO patients or indeed confer any prognostic value.

Cortical Topography of Atrophy in CO Intoxication Was Similar to the Behavior Variant of Frontotemporal Dementia

An intriguing feature seen in our CO degenerative networks was similar to that reported in the behavioral variant of frontotemporal degeneration.[48] It has been proposed that the degenerative network in frontotemporal dementia is initially targeted at the anterior insular region.[49] Similarly, the involvement of anterior insular regions was found in our patients, regardless of cognitive severity. Our patients with objective cognitive deficits (Group 2 and 3) that showed paralimbic system, anterior cingulate, dorsolateral, and frontoinsular region damage again showed a topography similar to that reported in patients with advanced frontotemporal dementia.[50] As the paralimbic region is anatomically linked with the anterior cingulate cortex, and functionally anchored with the frontoinsular region, comparisons between these 2 diseases with different pathological etiologies offer an insight into how the interconnected frontoinsular-subcortical networks undergo similar degenerative topography.

It is not known why the neuroimaging changes in CO intoxication follow the topographic distribution of frontotemporal dementia. The pathological process in CO intoxication patients was triggered by the exogenous toxic exposure to CO, as opposed to the endogenous genetic or molecular susceptibility to frontotemporal dementia.[51] These similarities may reflect common pathological pathway that leads to the topographic patterns in these 2 diseases.

LIMITATIONS

There are several limitations to this study. First, cerebral regional vulnerability to complex pathological reactions in CO encephalopathy can be highly individualized depending on the patients' immune status.[4–9] Therefore, our study results only represent structural and functional changes at a group level. Further studies with a larger number of patients are required to investigate interactions and weighting of each region that contribute to the wiring of the networks. Second, the reconstructed maps in this study were established at a chronic clinical stage and aimed to explore the neuronal injury pattern after reorganizational processes, and therefore this may not indicate a similar impact at the acute or delayed neuropsychiatric sequelae stages. Lastly, no histological evidence was available in this study because of the cross-sectional nature of studies involving human subjects. The interpretation of the degeneration theme was based on the current knowledge of pathophysiological meaning conveyed by the neuroimaging modalities and the histological evidence in CO intoxication.[6,13,52] It is worth noting that pathogenetic interactions among individual immune responses have not been conclusively established, and a longitudinal approach to topography degeneration may help validate our cross-sectional results.

CONCLUSION

In conclusion, our study suggests that with a longer follow-up period, acute CO intoxication would induce frontotemporal GM and WM degeneration that was cognitive severity specific. Structural alteration and related neuronal hypometabolism were highly correlated, reflecting a decompensatory process to the continuous intracellular stress. Damage to the prefrontal WM bundles and the major association fibers were related and were crucial in augmenting damage to the connecting cortical networks.

ACKNOWLEDGMENTS

The authors wish to thank the patients and their caregivers for their time and commitment to this research. We are also grateful to Drs TL Huang, PY Lin, Y Lee, and CH Lin from the Department of Psychiatry at the Kaohsiung Chang Gung Memorial Hospital for referring patients with carbon monoxide intoxication and Miss Lin YT for arranging all the experiments.

REFERENCES

1. Liu KY, Beautrais A, Caine E, et al. Charcoal burning suicides in Hong Kong and urban Taiwan: an illustration of the impact of a novel suicide method on overall regional rates. *J Epidemiol Community Health.* 2007;61:248–253.
2. Chang SS, Chen YY, Yip PS, et al. Regional changes in charcoal-burning suicide rates in East/Southeast Asia from 1995 to 2011: a time trend analysis. *PLoS Med.* 2014;11:e1001622.
3. Chang YT, Chang WN, Huang SH, et al. Neuroimaging Studies in Carbon Monoxide Intoxication. Slavka Krautzeka, Croatia: InTech; 2012.
4. Plum F, Posner JB, Hain RF. Delayed neurological deterioration after anoxia. *Arch Intern Med.* 1962;110:18–25.
5. Penney DG, Helfman CC, Dunbar JC Jr et al. Acute severe carbon monoxide exposure in the rat: effects of hyperglycemia and hypoglycemia on mortality, recovery, and neurologic deficit. *Can J Physiol Pharmacol.* 1991;69:1168–1177.
6. Lapresle J, Fardeau M. The central nervous system and carbon monoxide poisoning. II. Anatomical study of brain lesions following intoxication with carbon monixide (22 cases). *Prog Brain Res.* 1967;24:31–74.
7. Wagner KR, Kleinholz M, Myers RE. Delayed neurologic deterioration following anoxia: brain mitochondrial and metabolic correlates. *J Neurochem.* 1989;52:1407–1417.
8. Chang CC, Chang WN, Lui CC, et al. Longitudinal study of carbon monoxide intoxication by diffusion tensor imaging with neuropsychiatric correlation. *J Psychiatry Neurosci.* 2010;35:115–125.
9. Prockop LD, Chichkova RI. Carbon monoxide intoxication: an updated review. *J Neurol Sci.* 2007;262:122–130.
10. Piantadosi CA. Carbon monoxide poisoning. *N Engl J Med.* 2002;347:1054–1055.
11. Piantadosi CA, Zhang J, Levin ED, et al. Apoptosis and delayed neuronal damage after carbon monoxide poisoning in the rat. *Exp Neurol.* 1997;147:103–114.
12. Auer RN, Benveniste H. Carbon monoxide poisoning. In: Graham DI, Lantos PL, eds. *Greenfield's neuropathology.* London: Hodder Amold Publication; 1996. 275–276.
13. Lapresle J, Fardeau M. The leukoencephalopathies caused by carbon monoxide poisoning. Study of sixteen anatomo-clinical observations. *Acta Neuropathol.* 1966;6:327–348.
14. Chen NC, Chang WN, Lui CC, et al. Detection of gray matter damage using brain MRI and SPECT in carbon monoxide intoxication: a comparison study with neuropsychological correlation. *Clin Nucl Med.* 2013;38:e53–e59.
15. Durak AC, Coskun A, Yikilmaz A, et al. Magnetic resonance imaging findings in chronic carbon monoxide intoxication. *Acta Radiol.* 2005;46:322–327.

16. Gale SD, Hopkins RO, Weaver LK, et al. MRI, quantitative MRI, SPECT, and neuropsychological findings following carbon monoxide poisoning. *Brain Inj.* 1999;13:229–243.
17. Lee MS, Lyoo CH, Choi YH. Primary progressive freezing gait in a patient with CO-induced parkinsonism. *Mov Disord.* 2010;25:1513–1515.
18. Laplane D, Levasseur M, Pillon B, et al. Obsessive-compulsive and other behavioural changes with bilateral basal ganglia lesions. A neuropsychological, magnetic resonance imaging and positron tomography study. *Brain.* 1989;112 (Pt 3):699–725.
19. Moster ML, Galetta SL, Schatz NJ. Physiologic functional imaging in ''functional'' visual loss. *Surv Ophthalmol.* 1996;40:395–399.
20. Munoz Negrete FJ, Rebolleda G. Automated perimetry and neuro-ophthalmology. Topographic correlation. *Arch Soc Esp Oftalmol.* 2002;77:413–428.
21. Senol MG, Yildiz S, Ersanli D, et al. Carbon monoxide-induced cortical visual loss: treatment with hyperbaric oxygen four years later. *Med Princ Pract.* 2009;18:67–69.
22. Tengvar C, Johansson B, Sorensen J. Frontal lobe and cingulate cortical metabolic dysfunction in acquired akinetic mutism: a PET study of the interval form of carbon monoxide poisoning. *Brain Inj.* 2004;18:615–625.
23. Rissanen E, Paavilainen T, Virta J, et al. Carbon monoxide poisoning-induced nigrostriatal dopaminergic dysfunction detected using positron emission tomography (PET). *Neurotoxicology.* 2010;31:403–407.
24. Basser PJ, Pierpaoli C. Microstructural and physiological features of tissues elucidated by quantitative-diffusion-tensor MRI. *J Magn Reson B.* 1996;111:209–219.
25. Rorschach HE, Lin C, Hazlewood CF. Diffusion of water in biological tissues. *Scanning Microsc Suppl.* 1991;5:S1–S9discussion S9–S10.
26. Hua K, Zhang J, Wakana S, et al. Tract probability maps in stereotaxic spaces: analyses of white matter anatomy and tract-specific quantification. *Neuroimage.* 2008;39:336–347.
27. Fazio F, Perani D. Importance of partial-volume correction in brain PET studies. *J Nucl Med.* 2000;41:1849–1850.
28. Chen NC, Huang CW, Lui CC, et al. Diffusion-weighted imaging improves prediction in cognitive outcome and clinical phases in patients with carbon monoxide intoxication. *Neuroradiology.* 2013;55:107–115.
29. Folstein MF, Folstein SE, McHugh PR. ''Mini-mental state''. A practical method for grading the cognitive state of patients for the clinician. *J Psychiatr Res.* 1975;12:189–198.
30. Chang CC, Kramer JH, Lin KN, et al. Validating the Chinese version of the Verbal Learning Test for screening Alzheimer's disease. *J Int Neuropsychol Soc.* 2010;16:244–251.
31. Boone KB. The Boston Qualitative Scoring System for the Rey-Osterrieth Complex Figure. *J Clin Exp Neuropsychol.* 2000;22:430–434.
32. Kaplan EF, Goodglass H, Weintraub S. The Boston Naming Test. Philadelphia, PA: Lea & Febiger; 1983.
33. Warrington EK, James M. Visual Object and Space Perception Battery. Suffolk, UK: Thames Valley Test Co; 1991.
34. Chen NC, Chang CC, Lin KN, et al. Patterns of executive dysfunction in amnestic mild cognitive impairment. *Int Psychogeriatr.* 2013;25:1181–1189.
35. Chang CC, Lee YC, Chang WN, et al. Damage of white matter tract correlated with neuropsychological deficits in carbon monoxide intoxication after hyperbaric oxygen therapy. *J Neurotrauma.* 2009;26:1263–1270.
36. Muller-Gartner HW, Links JM, Prince JL, et al. Measurement of radiotracer concentration in brain gray matter using positron emission tomography: MRI-based correction for partial volume effects. *J Cereb Blood Flow Metab.* 1992;12:571–583.
37. Chang CC, Chang YY, Chang WN, et al. Cognitive deficits in multiple system atrophy correlate with frontal atrophy and disease duration. *Eur J Neurol.* 2009;16:1144–1150.
38. Good CD, Johnsrude IS, Ashburner J, et al. A voxel-based morphometric study of ageing in 465 normal adult human brains. *Neuroimage.* 2001;14:21–36.
39. Chang CC, Chang WN, Lui CC, et al. Clinical significance of the pallidoreticular pathway in patients with carbon monoxide intoxication. *Brain.* 2011;134:3632–3646.
40. Schmahmann JD, Pandya DN. The complex history of the fronto-occipital fasciculus. *J Hist Neurosci.* 2007;16:362–377.
41. Jang SH, Yeo SS. Thalamocortical tract between anterior thalamic nuclei and cingulate gyrus in the human brain: diffusion tensor tractography study. *Brain Imaging Behav.* 2013;7:236–241.
42. Schmahmann JD, Pandya DN. Disconnection syndromes of basal ganglia, thalamus, and cerebrocerebellar systems. *Cortex.* 2008;44:1037–1066.
43. Wedeen VJ, Wang RP, Schmahmann JD, et al. Diffusion spectrum magnetic resonance imaging (DSI) tractography of crossing fibers. *Neuroimage.* 2008;41:1267–1277.
44. Hurley RA, Hopkins RO, Bigler ED, et al. Applications of functional imaging to carbon monoxide poisoning. *J Neuropsychiatry Clin Neurosci.* 2001;13:157–160.
45. Gotoh M, Kuyama H, Asari S, et al. Sequential changes in MR images of the brain in acute carbon monoxide poisoning. *Comput Med Imaging Graph.* 1993;17:55–59.
46. Roohi F, Kula RW, Mehta N. Twenty-nine years after carbon monoxide intoxication. *Clin Neurol Neurosurg.* 2001;103:92–95.
47. Jack CR Jr, Albert MS, Knopman DS, et al. Introduction to the recommendations from the National Institute on Aging-Alzheimer's Association workgroups on diagnostic guidelines for Alzheimer's disease. *Alzheimers Dement.* 2011;7:257–262.
48. Seeley WW, Crawford R, Rascovsky K, et al. Frontal paralimbic network atrophy in very mild behavioral variant frontotemporal dementia. *Arch Neurol.* 2008;65:249–255.
49. Seeley WW, Zhou J, Kim EJ. Frontotemporal dementia: what can the behavioral variant teach us about human brain organization? *Neuroscientist.* 2012;18:373–385.
50. Seeley WW, Carlin DA, Allman JM, et al. Early frontotemporal dementia targets neurons unique to apes and humans. *Ann Neurol.* 2006;60:660–667.
51. Warren JD, Rohrer JD, Rossor MN. Clinical review. Frontotemporal dementia. *BMJ.* 2013;347:f4827.
52. Lapresle J, Fardeau M. Acute carbon monoxide poisoning. Anatomic study of an unusual encephalopathy caused by the diffusion of necrotic lesions and the importance of calcium deposits. *Bol Estud Med Biol.* 1971;27:9–17.